frontiers | Frontiers in Chemistry

TYPE Original Research
PUBLISHED 03 October 2022
DOI 10.3389/fchem.2022.983778

OPEN ACCESS

EDITED BY
David Raciti,
National Institute of Standards and Technology (NIST), United States

REVIEWED BY
Carla Casadevall Serrano,
University of Cambridge,
United Kingdom
Jiajun Wang,
Tianjin University, China

*CORRESPONDENCE
Miao Zhong,
miaozhong@nju.edu.cn

†These authors have contributed equally to this work

SPECIALTY SECTION
This article was submitted to Electrochemistry,
a section of the journal
Frontiers in Chemistry

RECEIVED 01 July 2022
ACCEPTED 15 September 2022
PUBLISHED 03 October 2022

CITATION
Li L, Jin X, Yu X and Zhong M (2022), Bimetallic Cu-Bi catalysts for efficient electroreduction of CO_2 to formate.
Front. Chem. 10:983778.
doi: 10.3389/fchem.2022.983778

Bimetallic Cu-Bi catalysts for efficient electroreduction of CO_2 to formate

Le Li†, Xuan Jin†, Xiaohan Yu and Miao Zhong*

National Laboratory of Solid State Microstructures, Jiangsu Key Laboratory of Artificial Functional Materials, College of Engineering and Applied Sciences, Nanjing University, Nanjing, China

Electrochemical CO_2 reduction offers an effective means to store renewable electricity in value-added chemical feedstocks. Much effort has been made to develop catalysts that achieve high Faradaic efficiency toward Formate production, but the catalysts still need high operating potentials to drive the CO_2–to–formate reduction. Here we report physical vapor deposition to fabricate homogeneously alloyed, compositionally controlled $Cu_{1-x}Bi_x$ bimetallic catalysts over a large area with excellent electrical conductivity. Operating electrochemical studies in Ar-saturated and CO_2-saturated electrolytes identified that Cu–Bi catalysts notably suppress the competing H_2 evolution reaction and enhance CO_2–to–formate selectivity. We reported a formate Faradaic efficiency of >95% at an improved cathodic potential of ~−0.72 V vs. RHE and a high formate cathodic energy efficiency of ~70%. The electrochemical reaction is stable over 24 h at a current density of 200 mA cm^{-2}. The work shows the advantages of bimetallic catalysts over single metal catalysts for increased reaction activity and selectivity.

KEYWORDS

electrocatalysis, Cu-Bi, bimetal, CO_2R, formate

Introduction

With the rapid development of modern society, the excessive burning of fossil fuels has led to huge amounts of CO_2 emissions, breaking the ecological carbon cycle and causing the growing greenhouse effect (Singh et al., 2016; Xiao et al., 2017; Garza et al., 2018; Birdja et al., 2019; Li et al., 2020). Renewably powered CO_2 conversion to value-added fuels or chemical raw materials, such as CO, $HCOO^-$, C_2H_4, C_2H_5OH, etc., is becoming an important way to maintain energy and environmental sustainability (Kortlever et al., 2015; Wang et al., 2021a; Wang et al., 2021b; Wang et al., 2022). For example, the electroreduction of CO_2 using renewable electricity has attracted great research attention (Wang et al., 2021c). Among the commonly reported CO_2R products, formic acid or formate stands out as a promising liquid chemical due to its high energy value in the techno-economic analysis and high volumetric mass density (53.4 g L^{-1}) for easy storage and transport (Yoo et al., 2016; Chi et al., 2021).

Conventionally, p block metals such as Bi, Pb, and In have appropriate *OCHO binding energy, favoring the CO_2–to–formate conversion. However, the electrical conductivity of these metals is not satisfactory, causing a large potential loss at high current densities. Cu is naturally abundant and has good electrical conductivity, possible for practical use (Huang et al., 2018). Cu-based materials are widely investigated as electrocatalysts for CO_2R to multi-carbon (C_{2+}) production (Mistry et al., 2016a; Mistry et al., 2016b; Gao et al., 2019; Zaza et al., 2022). However, due to the modest binding to H, C, and O (Qin et al., 2019; Zheng et al., 2021; Zhang et al., 2022), Cu shows poor selectivity to one specific product which leads to an increased product separation cost.

Bimetallic catalysts have been reported to increase the activity and selectivity of electrocatalytic CO_2R by taking the advantage of both metals. Zeng et al. improved the formate production by fabricating single atom Pb anchored Cu catalysts (Zheng et al., 2021); Thomas J. Meyer et al. enhanced selectivity for methane production by forming Cu-Pd bimetal alloys (Zhang et al., 2015); Douglas R. MacFarlane et al. improved the electrocatalytic reduction of CO_2 to CO by loading Au on Cu (Chen et al., 2017); Wang et al. (2010) prepared novel silver-coated nanoporous copper composite electrocatalysts for CO_2R to produce dimethyl carbonate. As for formate production, Bi is extensively studied as a promising CO_2R–to–formate catalyst due to its abundance on Earth, low cost, and environmental-benign properties. Jiang and collaborators reported that a Bi nanostructured catalyst electrochemically reduced by BiOCl nanosheets obtained 92% FE_{HCOOH} at −1.5 V vs. SCE at room temperature (Zhang et al., 2014); Zhong et al. achieved over 95% formate selectivity with ultra-long stability of more than 100 days (Li et al., 2021); Li et al. (2019) achieved nearly 100% formate selectivity using Bi/Bi_2O_3 with abundant grain boundaries as catalysts. Yet the Bi-based catalysts still require a high potential to conduct electrocatalytic reduction of CO_2 (Tian et al., 2021).

Herein, we present the large-area fabrication of $Cu_{1-x}Bi_x$ (x = 0.1, 0.2, 0.25) catalysts using controllable thermal evaporation. We evaluated the CO_2R and also the competing hydrogen evolution reaction (HER) performance in flow cells in CO_2-saturated and Ar-saturated electrolytes. We obtained a formate selectivity of 95% and a cathode energy efficiency of 70% at −0.72 V vs. RHE with $Cu_{0.8}Bi_{0.2}$. The CO_2R can proceed stably and efficiently at a current density of 200 mA cm^{-2} over 24 h. We conclude that the bimetallic $Cu_{0.8}Bi_{0.2}$ improves formate selectivity and enhances the CO_2R activity and cathodic energy efficiency, which may offer new perspectives for future design and synthesis of bimetallic CO_2R catalysts.

Experimental section

Synthesis of $Cu_{1-x}Bi_x$ (x = 0.1, 0.2, 0.25), Cu and Bi catalyst

$Cu_{1-x}Bi_x$ (x = 0.1, 0.2, 0.25), Cu, and Bi catalysts were synthesized by using the thermal evaporation (SKY-RH400) method. To prepare the $Cu_{1-x}Bi_x$ (x = 0.1, 0.2, 0.25) catalyst, the precursors Cu and Bi particles are evaporated onto the PTFE gas diffusion electrodes by thermal evaporation. In brief, 2 g of Bi metal particles and 2 g of Cu metal particles were put into the tungsten boats in the deposition chamber. The metal powder was slowly melted in a vacuum environment below $5*10^{-4}$ Pa. The evaporation rate of Bi was set to 0.03, 0.04, and 0.05 nm s^{-1} and Cu was set to 0.07, 0.06, and 0.05 nm s^{-1} to obtain $Cu_{1-x}Bi_x$ (x = 0.1, 0.2, 0.25) samples. The thickness of the as-deposited $Cu_{1-x}Bi_x$ (x = 0.1, 0.2, 0.25) films was about 500 nm as measured by a thickness meter placed inside the evaporation chamber. Uniform bimetallic films were obtained. To prepare the pure Bi and Cu films with the same thickness as control samples, we evaporated both Bi and Cu at 0.1 nm s^{-1} under the same conditions.

Characterization

Field Emission Scanning Electron Microscope (FESEM) images were taken on a SU8100 Scanning Electron Microscope. SEM-EDX test voltage is 20 kV. Powder X-ray diffraction (XRD) was performed using a Bruker D8 Advance X-ray diffractometer using Cu Kα radiation (λ = 0.15418 nm) in the 2θ range of 20°–80° at a scan rate of 7°/min. X-ray photoelectron spectroscopy (XPS) studies were performed using PHI5000 VersaProbe. The binding energy data were calibrated relative to the C 1s signal at 284.6 eV.

Electrochemical measurements

The electrochemical CO_2R experiments were carried out in a flow cell setup of a three-electrode system. The CO_2R catalysts, Ag/AgCl electrodes, and foamed nickel films were used as working electrodes, reference electrodes, and counter electrodes, respectively. 1 M KOH electrolytes were used as both catholyte and anolyte. An anion exchange membrane (Fumasep FAB-PK-130) was used to separate the catholyte and anolyte. All measurements were performed by using an electrochemical workstation (AOTU-Lab). All experiments were performed under the standard conditions with a CO_2 gas flow rate of 25 standard cubic centimeter per minute (sccm) at the flow cell outlet. The potential range of linear sweep voltammetry (LSV) is 0 to −1.2 V_{RHE}, with a sweep speed of 50 mV s^{-1}. The electrode potentials were converted to the RHE potentials using $V_{RHE} = V_{Ag/AgCl} + 0.197 + 0.059 \times$ pH. Electrochemical impedance spectroscopy (EIS) was measured at open circuit potential with amplitudes of 10 mV over the frequency range of 1 MHz to 1 Hz. The liquid products of CO_2 reduction were quantitatively analyzed by ion chromatography (Shenghan ICS-1000). Gaseous products were analyzed by gas chromatography

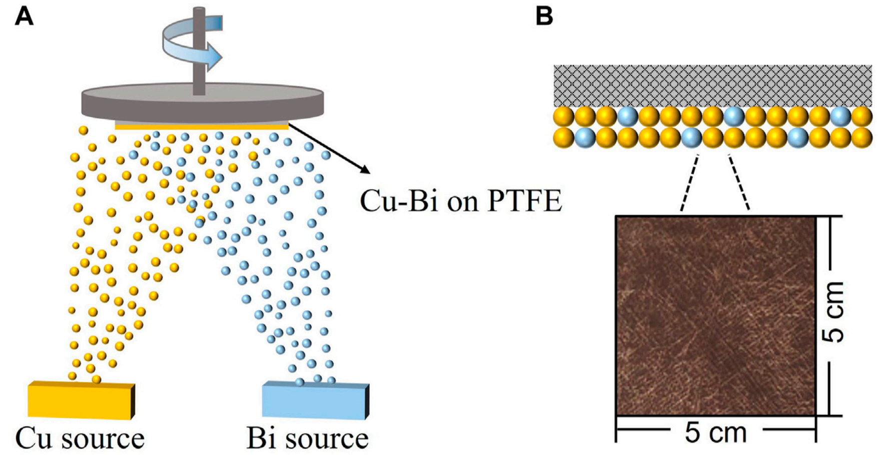

FIGURE 1
(A) A schematic illustration of the synthetic process of Cu-Bi catalyst on polytetrafluoroethylene (PTFE). **(B)** The insert optical image shows a 5 cm^2 × 5 cm^2 sample of $Cu_{0.8}Bi_{0.2}$ on the PTFE substrate.

(PE GC9790). ^1H nuclear magnetic resonance (NMR) spectroscopy was used to identify other liquid products other than formate. All measurements were made at room temperature and ambient pressure.

The Faradaic Efficiency (FE) of formate is calculated as follows:

$$FE_{formate} = \frac{n*F*V*c}{1000*M*Q}$$

where n is the number of electrons transferred (n = 2). F is Faraday's constant (96,485 C mol^{-1}). c is the mass concentration of formate produced by the reaction (mg L^{-1}). V is the volume of catholyte (L). M is the molar mass of formate (46.03 g mol^{-1}). Q is the total amount of charge consumed by the entire reaction monitored by the electrochemical workstation (C).

The FE of the gas product is calculated according to the following equation:

$$FE_{gas} = \frac{n*F*V}{1000*22.4*Q}$$

where n is the number of electrons transferred (n = 2). F is Faraday's constant (96,485 C mol^{-1}). V is the volume of catholyte (L). Q is the total amount of charge consumed by the entire reaction monitored by the electrochemical workstation (C).

Cathode Energy Efficiency (CEE) Calculation Formula:

$$CEE_{formate} = \frac{(1.23 - E_{formate})*FE_{formate}}{1.23 - E_{cathode}}$$

where $E_{formate}$ of −0.199 V vs. RHE is the standard potential of the formate formation. $FE_{formate}$ is the measured formate Faradaic efficiency. $E_{cathode}$ is the applied potential vs. RHE.

Results and discussion

We prepared a series of $Cu_{1-x}Bi_x$ (x = 0.1, 0.2, 0.25) bimetallic materials, pure Cu, and pure Bi samples on a large area by thermal evaporation. As shown in Figures 1A,B and Supplementary Figure S1, the as-prepared $Cu_{1-x}Bi_x$ (x = 0.1, 0.2, 0.25) catalysts were all tightly wrapped on the PTFE fibers and formed uniformly distributed Cu and Bi nanoparticles with a size of 100–200 nm. It can be seen from Figure 2A and Supplementary Figure S1 that with the increase of Bi content, the particles gradually form nanocrystals, and the particle size of $Cu_{1-x}Bi_x$ (x = 0.1, 0.2, 0.25) is about 100–200 nm, and the Cu-Bi bimetallic distribution is uniform. The particle sizes of Bi and Cu are 200 nm and 50–100 nm, respectively. Then we measured the element distribution using SEM-EDX. As shown in the mapping spectrum, Cu and Bi elements were uniformly distributed on the catalyst surfaces (Figures 2B,C; Supplementary Figure S2). Through SEM-EDX and XPS analysis, the element ratio of our prepared Cu-Bi was 0.8:0.2 (Supplementary Figure S3).

The chemical states of the synthesized Cu, $Cu_{0.8}Bi_{0.2}$, and Bi catalysts were studied by the high-resolution XPS spectra of Bi 4f and Cu 2p, respectively (Figures 3A,B). We observed that the strong peaks at 158.7 and 164.0 eV corresponded to Bi^{3+} $4f_{7/2}$ and Bi^{3+} $4f_{5/2}$, and the peaks at 157.0 eV, 162.3 eV corresponded to Bi^0 $4f_{7/2}$ and Bi^0 $4f_{5/2}$. From the high-resolution XPS spectrum of Cu 2p, the peaks at 932.0 and 951.8 eV corresponded to $Cu^{0,\,1+}$, while the peaks at 933.9 and 953.6 eV were consistent with Cu^{2+}. It should be explained that both Cu and Bi are easily oxidized in air, the positively charged Bi^{3+} and Cu^{2+} are detected, probably because the oxidation occurred during the storage of the sample in air. Compared with Cu, the d-band center of $Cu_{0.8}Bi_{0.2}$ moved more positively after the introduction of Bi

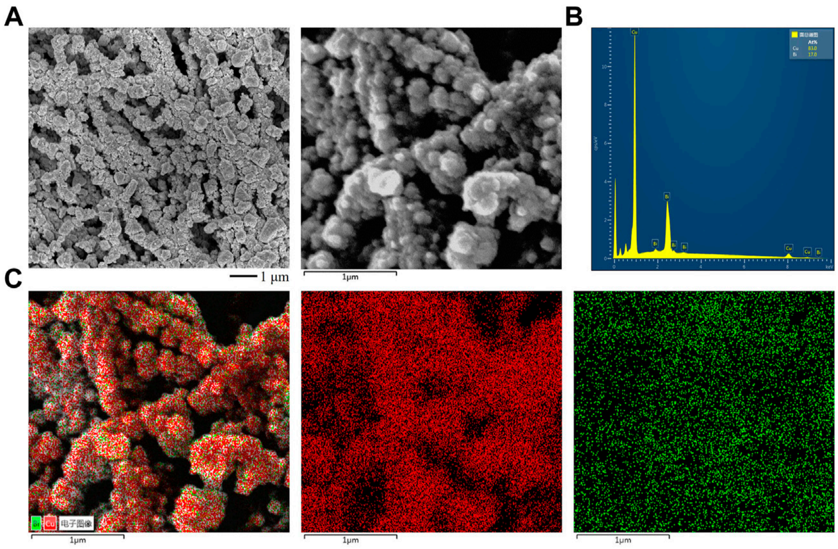

FIGURE 2
(A) SEM images of the synthesized $Cu_{0.8}Bi_{0.2}$ by thermal evaporation. **(B)** EDX spectrum of the $Cu_{0.8}Bi_{0.2}$. **(C)** EDX Mapping results of the $Cu_{0.8}Bi_{0.2}$.

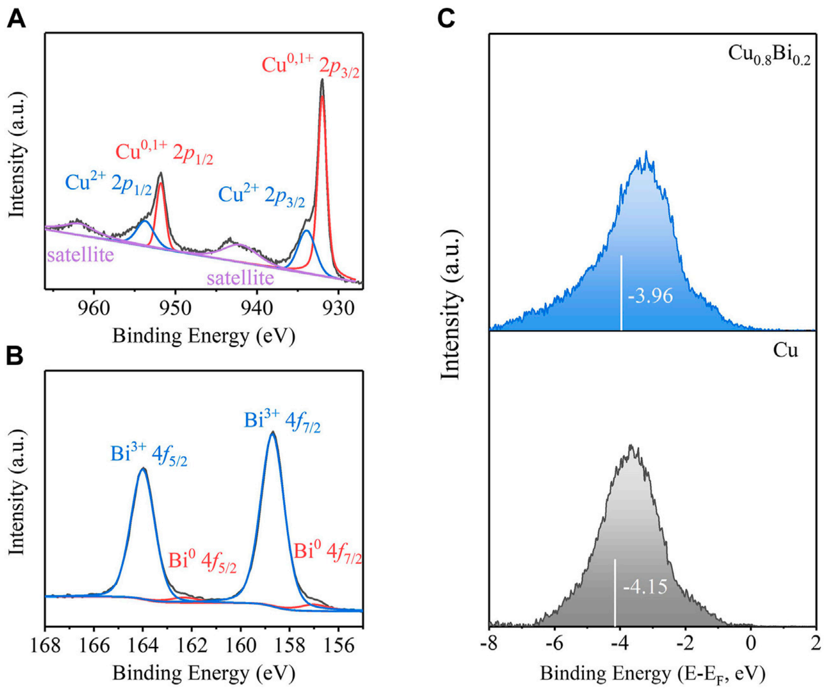

FIGURE 3
(A) Cu 2p XPS spectra of $Cu_{0.8}Bi_{0.2}$. **(B)** Bi 4f XPS spectra of $Cu_{0.8}Bi_{0.2}$. **(C)** Surface valence band photoemission spectra of Cu and $Cu_{0.8}Bi_{0.2}$. The white bar in **(C)** highlights the *d*-band center of various materials.

species (Figure 3C). As reported, the positively shifted d-band center likely increases the electron donation from the catalysts to the adsorbed *OCHO intermediate, strengthening the *OCHO surface binding (Xin et al., 2014; Zhang et al., 2018). This is consistent with our electrochemical CO_2R test that Cu-Bi catalysts show improved performance.

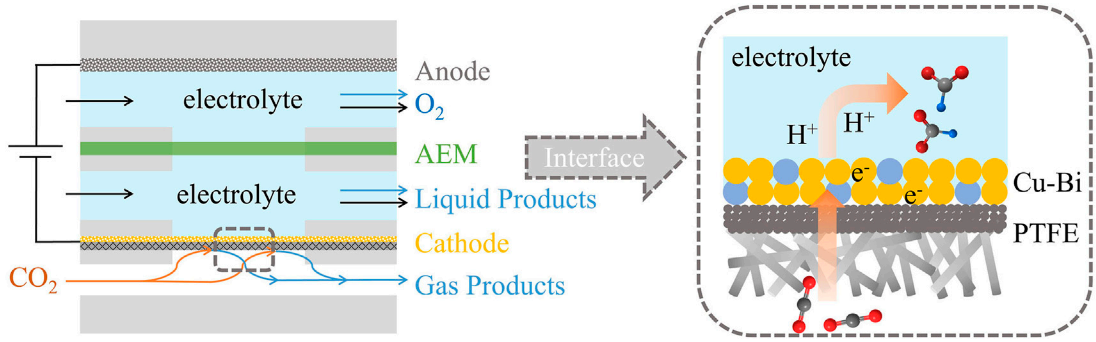

FIGURE 4
Schematic of Cu-Bi electrocatalyst on PTFE for electroreduction of CO_2 in a flow cell.

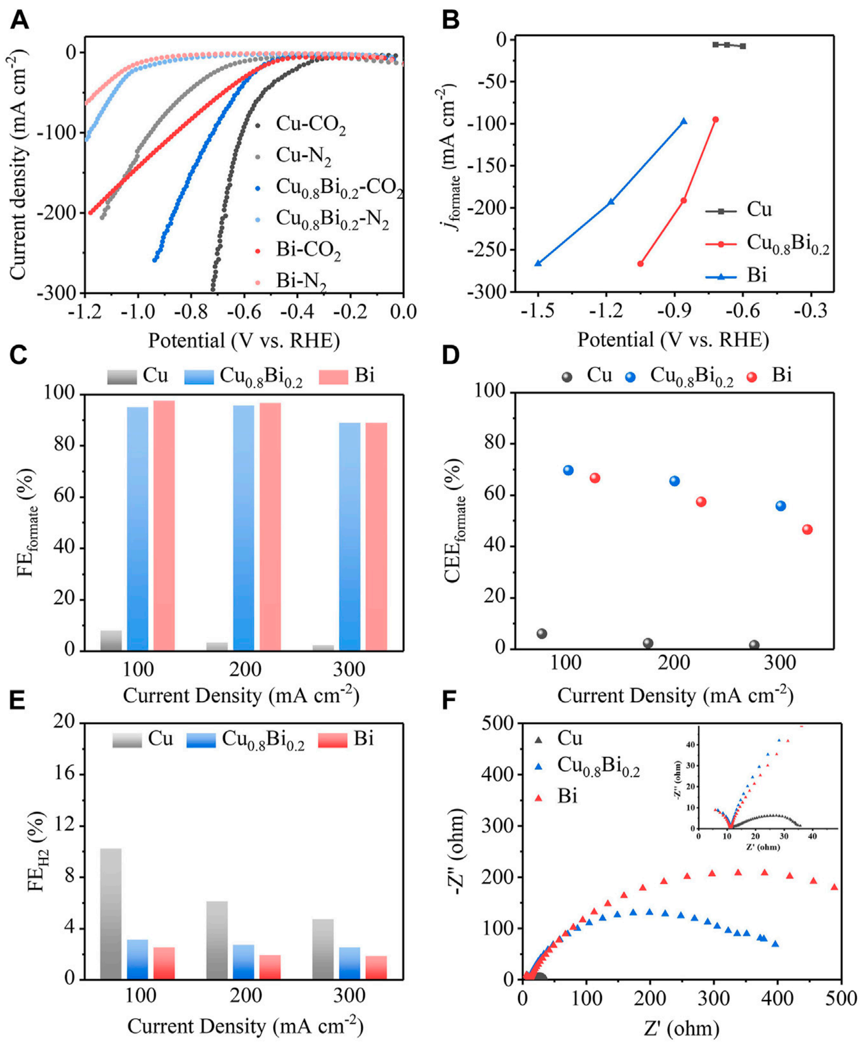

FIGURE 5
(A) The LSV curves under CO_2 or N_2 conditions of $Cu_{0.8}Bi_{0.2}$, Cu, and Bi. **(B)** The particular current density of formate of $Cu_{0.8}Bi_{0.2}$, Cu, and Bi. **(C,E)** The faradaic efficiency of formate and H_2 of $Cu_{0.8}Bi_{0.2}$, Cu, and Bi at current densities of 100, 200, and 300 mA cm^{-2}. **(D)** The cathode energy efficiency of formate at current densities of $Cu_{0.8}Bi_{0.2}$, Cu, and Bi of 100, 200, and 300 mA cm^{-2}. **(F)** The EIS curve of Cu, $Cu_{0.8}Bi_{0.2}$, and Bi.

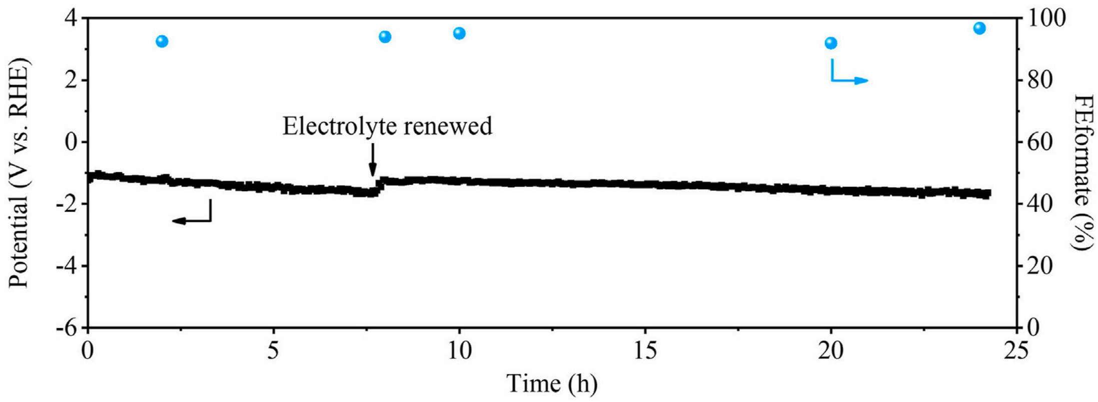

FIGURE 6
The stability test of $Cu_{0.8}Bi_{0.2}$ in 1 M KOH at 200 mA cm^{-2}.

The CO_2R electrochemical performance of the $Cu_{1-x}Bi_x$ (x = 0.1, 0.2, 0.25), pure Cu, and pure Bi catalysts were tested in a flow cell with a three-electrode system (Figure 4). The anode was Ni, the reference electrode was an Ag/AgCl electrode, and the electrolyte was 1 M KOH solution (pH = 14). From the linear sweep voltammetry (LSV), we can intuitively see that the reaction overpotential of Cu-Bi bimetal was reduced significantly (Figure 5A; Supplementary Figure S4). As shown in Figure 3B, the overpotential (520 mV) of the $Cu_{0.8}Bi_{0.2}$ catalyst is significantly smaller than that of the Bi catalyst (660 mV) at the same current density (100 mA cm^{-2}). The overpotential for Cu is the best (400 mV), but the product selectivity is poor (Figure 5B). The cathodic current density on Cu, $Cu_{0.8}Bi_{0.2}$, and Bi electrodes was largely reduced when N_2 was passing through (Figure 5A). In the presence of N_2, the current density started to increase slowly at −0.70 V vs. RHE, which was mainly caused by the hydrogen evolution reaction (HER). It is also clear that HER on the Cu electrode is worse than CO_2R on the Bi electrode, indicating that the introduction of Bi into Cu can suppress HER In the presence of CO_2, which is more beneficial to CO_2R.

To investigate the product selectivity of CO_2R with $Cu_{0.8}Bi_{0.2}$, Cu, and Bi catalysts, chronopotentiometry tests were performed at current densities of 100, 200, and 300 mA cm^{-2}, respectively (Supplementary Figure S5). The products were quantitatively analyzed by gas chromatography (GC), ion chromatography (IC), and nuclear magnetic resonance (NMR). As shown in Figures 5C-E, and Supplementary Figure S6, the $Cu_{0.8}Bi_{0.2}$ catalyst achieved over 90% selectivity to formate at all current densities, in particular, the selectivity for formate reached 95% at a current density of 100 mA cm^{-2}, with a cathode energy efficiency reaching about 70%. Although the single-metal Bi catalyst has a formate selectivity close to that of $Cu_{0.8}Bi_{0.2}$, its cathode energy efficiency is much lower than that of $Cu_{0.8}Bi_{0.2}$ at all current densities due to its high reaction potential. In the case of the Cu catalyst, the formate selectivity is very low. Considering both the selective and energy efficiency, $Cu_{0.8}Bi_{0.2}$ outperforms Bi and Cu in the electroreduction of CO_2 to formate.

As shown in Figure 5E, we found that the introduction of Bi into Cu can significantly reduce HER, which is consistent with the LSV results under N_2 environment. To explain the reason for the excellent performance of $Cu_{0.8}Bi_{0.2}$ catalysts, we performed EIS tests on the three samples. As is shown in Figure 5F, $Cu_{0.8}Bi_{0.2}$ shows a smaller semicircle diameter than Bi in the impedance spectrum, suggesting that the charge transfer resistance of $Cu_{0.8}Bi_{0.2}$ is lower than that of Bi, ensuring a faster electron transfer during the reaction. The conductivity of Cu is 58.13953 S/m, and that of Bi is 0.95238 S/m. The conductivity of Cu is significantly better than that of Bi. Therefore, we analyze that the loading of Cu metal increases the conductivity of the material and reduces the charge transfer resistance, also the HER is greatly suppressed in the presence of CO_2, as a result, $Cu_{0.8}Bi_{0.2}$ can reduce the reaction overpotential and maintain high CO_2R catalytic activity and selectivity.

To verify the stability of the $Cu_{0.8}Bi_{0.2}$ catalyst, we performed the stability test at a current density of 200 mA cm^{-2}, and SEM characterization of the reacted sample was performed. It can be seen from Figure 6 that during the reaction process of the 24 h CO_2 reduction, the reaction potential did not change significantly, and the selectivity of $HCOO^-$ was maintained above 90%. We also carried out SEM, SEM-EDX, and XRD analyses of the sample after 24 h of reaction. From Supplementary Figure S7, we can observe that the morphology and structure of the $Cu_{0.8}Bi_{0.2}$ bimetallic catalyst did not change after the reaction. The XRD characterizations also showed that the catalyst did not change significantly after the reaction, indicating that good stability with $Cu_{0.8}Bi_{0.2}$ for CO_2R.

Conclusion

In conclusion, we developed a simple, controllable, and large-area preparation method for the synthesis of $Cu_{0.8}Bi_{0.2}$ catalysts. $Cu_{0.8}Bi_{0.2}$ exhibited excellent formate selectivity and cathode energy efficiency under all current densities. Specifically, it exhibited a formate selectivity of 95% and a cathode energy efficiency of 70% at a potential of −0.72 V vs. reversible hydrogen electrode and maintained the CO_2R durability for over 24 h at a current density of 200 mA cm^{-2}. The excellent catalytic performance of $Cu_{0.8}Bi_{0.2}$ is attributed to the following factors: 1) CuBi alloy likely has a favorable work function to improve CO_2 adsorption for formate production; 2) CuBi alloy improves electron transport. We expect that the bimetal $Cu_{0.8}Bi_{0.2}$ electrocatalyst may offer a material foundation for the improved catalytic CO_2R to formate conversion.

Data availability statement

The original contributions presented in the study are included in the article/Supplementary Material, further inquiries can be directed to the corresponding author.

Author contributions

MZ supervised the project. MZ conceived the idea and designed the experiments. LL and XJ conducted the synthesis, characterizations, and flow-cell tests. LL, XJ, XY, and MZ discussed the experiment results. MZ, XY, and LL wrote the manuscript. All authors discussed the results and assisted during manuscript preparation.

Funding

This work was supported by the National Key R&D Program of China (No. 2020YFA0406102), the National Natural Science Foundation of China (grant numbers 22272078 and 91963121), the Frontiers Science Center for Critical Earth Material Cycling of Nanjing University, and the “Innovation and Entrepreneurship of Talents plan” of Jiangsu Province.

Acknowledgments

The authors also acknowledge the support from Jiangsu Key Laboratory of nanotechnology, Nanjing University

Conflict of interest

The authors declare that the research was conducted in the absence of any commercial or financial relationships that could be construed as a potential conflict of interest.

Publisher's note

Supplementary material

The Supplementary Material for this article can be found online at: https://www.frontiersin.org/articles/10.3389/fchem.2022.983778/full#supplementary-material

References

Birdja, Y. Y., Perez-Gallent, E., Figueiredo, M. C., Gottle, A. J., Calle-Vallejo, F., and Koper, M. T. M. (2019). Advances and challenges in understanding the electrocatalytic conversion of carbon dioxide to fuels. *Nat. Energy* 4, 732–745. doi:10.1038/s41560-019-0450-y

Chen, K., Zhang, X., Williams, T., Bourgeois, L., and MacFarlane, D. R. (2017). Electrochemical reduction of CO_2 on core-shell Cu/Au nanostructure arrays for syngas production. *Electrochim. Acta* 239, 84–89. doi:10.1016/j.electacta.2017.04.019

Chi, L.-P., Niu, Z. Z., Zhang, X. L., Yang, P. P., Liao, J., Gao, F. Y., et al. (2021). Stabilizing indium sulfide for CO_2 electroreduction to formate at high rate by zinc incorporation. *Nat. Commun.* 12, 5835. doi:10.1038/s41467-021-26124-y

Gao, D., Arán-Ais, R. M., Jeon, H. S., and Roldan Cuenya, B. (2019). Rational catalyst and electrolyte design for CO_2 electroreduction towards multicarbon products. *Nat. Catal.* 2, 198–210. doi:10.1038/s41929-019-0235-5

Garza, A. J., Bell, A. T., and Head-Gordon, M. (2018). Mechanism of CO_2 reduction at copper surfaces: Pathways to C2 products. *ACS Catal.* 8, 1490–1499. doi:10.1021/acscatal.7b03477

Huang, Y., Deng, Y., Handoko, A. D., Goh, G. K. L., and Yeo, B. S. (2018). Rational design of sulfur-doped copper catalysts for the selective electroreduction of carbon dioxide to formate. *ChemSusChem* 11, 320–326. doi:10.1002/cssc.201701314

Kortlever, R., Shen, J., Schouten, K. J. P., Calle-Vallejo, F., and Koper, M. T. M. (2015). Catalysts and reaction pathways for the electrochemical reduction of carbon dioxide. *J. Phys. Chem. Lett.* 6, 4073–4082. doi:10.1021/acs.jpclett.5b01559

Li, J., Kuang, Y., Meng, Y., Tian, X., Hung, W. H., Zhang, X., et al. (2020). Electroreduction of CO_2 to formate on a copper-based electrocatalyst at high pressures with high energy conversion efficiency. *J. Am. Chem. Soc.* 142, 7276–7282. doi:10.1021/jacs.0c00122

Li, L., Ma, D.-K., Qi, F., Chen, W., and Huang, S. (2019). Bi nanoparticles/Bi_2O_3 nanosheets with abundant grain boundaries for efficient electrocatalytic CO_2 reduction. *Electrochim. Acta* 298, 580–586. doi:10.1016/j.electacta.2018.12.116

Li, L., Ozden, A., Guo, S., Garci´a de Arquer, F. P., Wang, C., Zhang, M., et al. (2021). Stable, active CO_2 reduction to formate via redox-modulated stabilization of active sites. *Nat. Commun.* 12, 5223. doi:10.1038/s41467-021-25573-9

Mistry, H., Varela, A. S., Bonifacio, C. S., Zegkinoglou, I., Sinev, I., Choi, Y. W., et al. (2016). Highly selective plasma-activated copper catalysts for carbon dioxide reduction to ethylene. *Nat. Commun.* 7, 12123. doi:10.1038/ncomms12123

Mistry, H., Varela, A. S., Kühl, S., Strasser, P., and Cuenya, B. R. (2016). Nanostructured electrocatalysts with tunable activity and selectivity. *Nat. Rev. Mat.* 1, 16009. doi:10.1038/natrevmats.2016.9

Qin, T., Qian, Y., Zhang, F., and Lin, B.-L. (2019). Cloride-derived copper electrode for efficient electrochemical reduction of CO_2 to ethylene. *Chin. Chem. Lett.* 30, 314–318. doi:10.1016/j.cclet.2018.07.003

Singh, M. R., Kwon, Y., Lum, Y., Ager, J. W., and Bell, A. T. (2016). Hydrolysis of electrolyte cations enhances the electrochemical reduction of CO_2 over Ag and Cu. *J. Am. Chem. Soc.* 138, 13006–13012. doi:10.1021/jacs.6b07612

Tian, J., Wang, R., Shen, M., Ma, X., Yao, H., Hua, Z., et al. (2021). Bi–Sn oxides for highly selective CO_2 electroreduction to formate in a wide potential window. *ChemSusChem* 14, 2247–2254. doi:10.1002/cssc.202100543

Wang, J., Wang, G., Zhang, J., Wang, Y., Wu, H., Zheng, X., et al. (2021). Inversely tuning the CO_2 electroreduction and hydrogen evolution activity on metal oxide via heteroatom doping. *Angew. Chem. Int. Ed. Engl.* 60, 7680–7684. doi:10.1002/ange.202016022

Wang, J., Zheng, X., Wang, G., Cao, Y., Ding, W., Zhang, J., et al. (2022). Defective bimetallic selenides for selective CO_2 electroreduction to CO. *Adv. Mat.* 34, e2106354. doi:10.1002/adma.202106354

Wang, J-J., Li, X-P., Cui, B-F., Zhang, Z., Hu, X-F., Ding, J., et al. (2021). A review of non-noble metal-based electrocatalysts for CO_2 electroreduction. *Rare Met.* 40, 3019–3037. doi:10.1007/s12598-021-01736-x

Wang, X., Ou, P., Wicks, J., Xie, Y., Wang, Y., Li, J., et al. (2021). Gold-in-copper at low *CO coverage enables efficient electromethanation of CO_2. *Nat. Commun.* 12, 3387. doi:10.1038/s41467-021-23699-4

Wang, X. Y., Liu, S. Q., Huang, K. L., Feng, Q. J., Ye, D. L., Liu, B., et al. (2010). Fixation of CO_2 by electrocatalytic reduction to synthesis of dimethyl carbonate in ionic liquid using effective silver-coated nanoporous copper composites. *Chin. Chem. Lett.* 21, 987–990. doi:10.1016/j.cclet.2010.04.022

Xiao, H., Cheng, T., and Goddard, W. A. (2017). Atomistic mechanisms underlying selectivities in C1 and C2 products from electrochemical reduction of CO on Cu (111). *J. Am. Chem. Soc.* 139, 130–136. doi:10.1021/jacs.6b06846

Xin, H., Vojvodic, A., Voss, J., Nørskov, J. K., and Abild-Pedersen, F. (2014). Effects ofd-band shape on the surface reactivity of transition-metal alloys. *Phys. Rev. B* 89, 115114. doi:10.1103/physrevb.89.115114

Yoo, J. S., Christensen, R., Vegge, T., Nørskov, J. K., and Studt, F. (2016). Theoretical insight into the trends that guide the electrochemical reduction of carbon dioxide to formic acid. *ChemSusChem* 9, 358–363. doi:10.1002/cssc.201501197

Zaza, L., Rossi, K., and Buonsanti, R. (2022). Well-defined copper-based nanocatalysts for selective electrochemical reduction of CO_2 to C2 products. *ACS Energy Lett.* 7, 1284–1291. doi:10.1021/acsenergylett.2c00035

Zhang, H., He, C., Han, S., Du, Z., Wang, L., Yun, Q., et al. (2022). Crystal facet-dependent electrocatalytic performance of metallic Cu in CO_2 reduction reactions. *Chin. Chem. Lett.* 33, 3641–3649. doi:10.1016/j.cclet.2021.12.018

Zhang, H., Ma, Y., Quan, F., Huang, J., Jia, F., and Zhang, L. (2014). Selective electro-reduction of CO_2 to formate on nanostructured Bi from reduction of BiOCl nanosheets. *Electrochem. Commun.* 46, 63–66. doi:10.1016/j.elecom.2014.06.013

Zhang, N., Jalil, A., Wu, D., Chen, S., Liu, Y., Gao, C., et al. (2018). Refining defect states in $W_{18}O_{49}$ by Mo doping: A strategy for tuning N_2 activation towards solar-driven nitrogen fixation. *J. Am. Chem. Soc.* 140, 9434–9443. doi:10.1021/jacs.8b02076

Zhang, S., Kang, P., Bakir, M., Lapides, A. M., Dares, C. J., and Meyer, T. J. (2015). Polymer-supported CuPd nanoalloy as A synergistic catalyst for electrocatalytic reduction of carbon dioxide to methane. *Proc. Natl. Acad. Sci. U. S. A.* 112, 15809–15814. doi:10.1073/pnas.1522496112

Zheng, T., Liu, C., Guo, C., Zhang, M., Li, X., Jiang, Q., et al. (2021). Copper-catalysed exclusive CO_2 to pure formic acid conversion via single-atom alloying. *Nat. Nanotechnol.* 16, 1386–1393. doi:10.1038/s41565-021-00974-5